Cored intervals from the Lower Cretaceous Hosston sandstone show sedimentary structures typical of fluvial and deltaic environments. The present depth of burial of the sandstone is 4,300 to 5,500 m (14,100 to 18,050 ft).

Selected samples of the sandstones were analyzed by petrographic, X-ray diffraction, scanning electron microscopy, and other methods to determine the composition and texture of the detrital and authigenic phases, diagenetic sequence, and the relation of facies, diagenesis, and reservoir rock properties.

The sandstones are fine grained, well sorted, and composed on the average of 68% quartz, 17% lithic fragments, 2% feldspars, 7% matrix, and 6% other minerals. Cements include silica and carbonate, which respectively constitute 8% and 9% of the bulk sample in general. Silica cement dominates in the fluvial facies, carbonate cement in the deltaic sandstones.

Alteration of rock fragments and feldspars results in clay authigenesis which accounts for practically all of the <0.01 mm size fraction in the sandstones. Coarsely crystalline kaolinite makes up 51% of the clays, illite 42%, and chlorite 6%. Kaolinite alters to illite as a function of temperature increase. While kaolinite is pore-filling, illite and chlorite are pore-lining.

The sandstones have an overall average porosity of 4.2%; the fluvial facies generally has porosities below average, the deltaic facies above. Intergranular pores and oversized pores are the dominant porosity types; both have developed by dissolution of cement or detrital grains. The deltaic facies exhibits inverse relation between porosity and total cement content. Because of the persistent presence of authigenic clays in the pores, microporosity forms a significant portion of total porosity, especially in the fluvial facies.

Permeability of the Hosston sandstones ranges from less than 0.01 md to slightly more than 5 md, the average being between 0.1 and 0.2 md. Thin sandstones of fluvial origin, which have microporosity, show lowest permeability, whereas sandstones of deltaic origin in nearby areas have high permeabilities primarily because of dissolution of grains and carbonate cement. Future exploration in the Hosston should, therefore, be directed to the deltaic sandstone.

WISE, D. U., D. GREENE, and M. VALENTINE, Univ. Massachusetts, Amherst, MA, and S. SCHAMEL*, S. PERRY, and H. ABU ZIED, Univ. South Carolina, Columbia, SC

Tectonic Trends, Timing, and Mechanics of the Egyptian Edge of the Red Sea and Gulf of Suez

Two major areas of onshore preservation of both pre- and syn-Red Sea sediments occur at Gebel Zeit, near the mouth of the Gulf of Suez, and at Quseir, 200 km (125 mi) to the south. At Quseir, a belt of 600 m.y. greenstone basement has at least three stages of coaxial N30°W deformation curving northwestward into N60°W grain of the regional Hamrawein Synclinorium. In Late Eocene (?) to Early Miocene time, this northwest-trending structure was further downwarped by block faulting with associated local gravity fold tectonics. The Cenozoic synclinorium dies out southeastward into a synchronous or slightly older system of north-south trending fault blocks, many of which show early stage right-lateral strike-slip slickenslides.

In the Mid-Miocene, the Red Sea coast suffered major downwarping along N25°W trends, whereas the interior synclinorium was further broken into generally northwest-trending, northeast-tilted irregular fault blocks reactivating many older fault trends.

By contrast, the Gebel Zeit block appears rigidly parallel with the N25°W Red Sea–Gulf of Suez trend and shows systematic long-term tilting away from the Gulf of Suez with at least five stages of Eocene through Miocene uplift, erosion of its eastern basement edge, and concomitant sinking and deposition on its western edge.

The evidence points to early stage fault patterns "inherited" from the local structural grain of the Precambrian basement that pre-dated the principal Red Sea–Gulf of Suez evolution into its dominant N25°W tectonic trend during the Miocene.

WITHJACK, MARTHA OLIVER, Cities Service Technology Center, Tulsa, OK, and D. J. DRICKMAN POLLOCK, Dallas, TX

Seismic Reflection Models of Rift-Related Structures

Published field data from several rifted basins indicate that normal faults and associated secondary structures (i.e., minor normal faults, folds produced by drag on fault surfaces, forced folds above faults) are common in rifts. The dip and curvature of the fault surfaces, the fault displacements, the dip of the strata within the fault blocks, and the position and size of the folds vary considerably. Our two-dimensional, seismic-reflection models systematically show how each of these variables, as well as rock velocity, influence the seismic expression of rift-related structures. These seismic models reveal several "pitfalls" of seismic interpretation common to rifts, many of which we have recognized on actual seismic data.

The observed dip and curvature of any fault surface on our unmigrated seismic models depend, not only on the dip and curvature of the actual fault surface, but also on the dip and velocity of the adjacent beds. The observed dip of a fault decreases as the angle between the actual fault surface and strata decreases. For example, normal faults dipping in the opposite direction as the strata appear to have greater dips than identical normal faults dipping in the same direction as the strata. Also, normal faults active during deposition (with beds on the downthrown side having increasing dip toward the faults with depth) appear to steepen

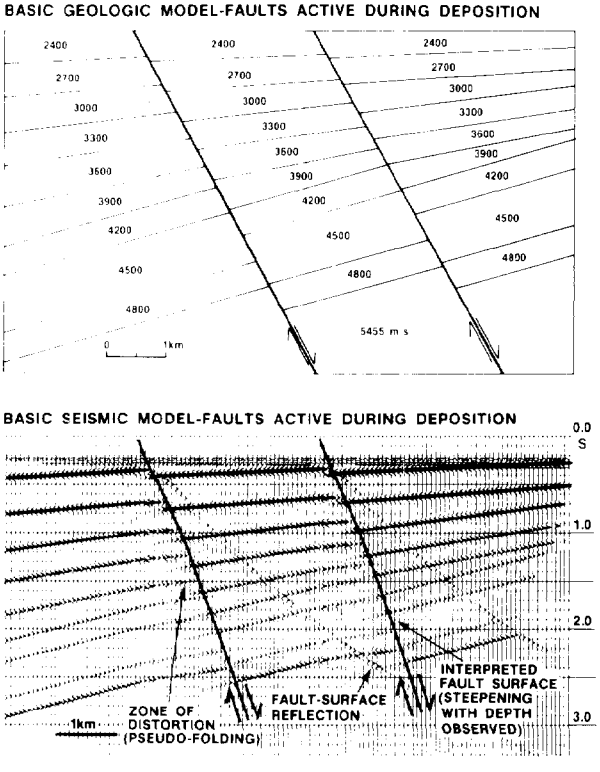

with depth more so than identical normal faults active after deposition. The observed dip of a fault decreases as the velocity of the adjacent rock increases. For example, normal faults in rocks whose velocities increase with depth (e.g., most clastic sedimentary rocks) appear to flatten with depth more so than identical normal faults in rocks with more uniform velocities.

The appearance of secondary structures associated with normal faulting on our unmigrated seismic models depends on the position and size of the secondary structures. The increased thickness of low-velocity rock on the downthrown side of normal faults disrupts and bends the reflections on the upthrown side. Depth, fault displacement rock velocity distribution, and the angle between the fault surface and adjacent beds affect the severity of the distortion. This distortion obscures any secondary structures present on the upthrown side of faults (i.e., minor faults, anticlines produced by drag) and can erroneously be interpreted as secondary faulting and folding. Synclines produced by drag on the downthrown side of normal faults have small radii of curvature relative to their burial depths. This relationship makes these synclines difficult to identify on unmigrated seismic sections. Many forced folds in rifts are gentle shallow structures overlying normal faults. These folds are the most easily identifiable because they are unaffected by the distortion beneath faults and the synclines have large radii of curvature compared to their burial depths.

WOODSIDE, PHILLIP R., Texas Eastern, Houston, TX

Petroleum Geology of Bangladesh

The easternmost part of the Bengal foredeep or Surma basin is the most prospective area for finding additional gas because the degree of folding diminishes markedly in a westward direction. The foothills of the Tripura-Chittagong area and the Bengal basin (sometimes called Bengal foredeep or Surma basin) are locations of the gas fields in Bangladesh. These areas have sometimes been called the Outer Molasse basin. Folding occurred in four phases. Gas discoveries are in the Chittagong foothills. Similar structural features to those of the Chittagong foothills appear to be present in the extreme eastern part of the Bay of Bengal. Compressional folding did not affect the central and western part of the Bay of Bengal. However, by comparison with other areas of deltaic deposition, rollover structures associated with growth faults may be significant. The Oligocene to Holocene rock sequences were deposited in environments that range from abyssal marine prodelta to subaerial delta plain. In productive areas onshore and offshore, hydrocarbon traps include asymmetric, elongate, faulted anticlines. Strategic traps and sedimentary growth structures are found in the Bengal basin. Miocene sandstones constitute the gas reservoirs; Eocene, Paleocene, and Oligocene carbonaceous shales and Miocene shales are the source rocks. In the central and western part of the Bay of Bengal area, the major uncertainties are the development and thickness of sandstones and the possible size of structures.

Thirteen gas fields have been discovered: (1) Kutubdia, (2) Chhatak (8 mmcf/day), (3) Kailashtilla, (4) Habiganj (14 mmcf/day), (5) Bakhrabad, (6) Murdi, (7) Begumgoni, (8) Beanibazar, (9) Sylhet, (10) Rashidpur, (11) Titas, (12) Semutang, and (13) Jaldi. Chhatak, Habiganj, Sylhet, and Titas fields were on production during 1979.

The gas in these fields occurs in multi-sandstone reservoirs in anticlines that probably developed in late Miocene to Pliocene time. The gas reservoirs are the lower Miocene Bhuban Formation and lower to lower-middle Miocene Boka Bil Formation. Both formations are included in the Surma Group.

Total recoverable gas reserves are 7 to 7.8 tcf. Total estimated gas reserves in place are 9.33 to 10.39 tcf and possibly 10 to 20 tcf of gas resources yet to be discovered.

WOODWARD, LEE A., Univ. New Mexico, Albuquerque, NM

Raton Basin, New Mexico—Exploration Frontier for Fracture Reservoirs in Cretaceous Shales

The Raton basin contains up to 3,000 ft (900 m) of marine shale and subordinate carbonate rocks of Cretaceous age, including (in ascending order) the Graneros Shale, Greenhorn Limestone, Carlile Shale, Niobrara Formation, and Pierre Shale. Clastic reservoir rocks are sparse in this part of the section and drilling for them in the Raton basin has led to disappointing results. However, brittle siltstone and carbonate-rich interbeds within the Cretaceous shale intervals are capable of providing fracture reservoirs under the right conditions.

Fracture reservoirs in other Rocky Mountain basins occur where there is maximum curvature of brittle interbeds within shale sequences at fairly shallow depths. Relatively low confining pressures found at shallow depth facilitate development of open fractures in the brittle interbeds. Anticlines, synclines, and monoclines can have favorable fracture systems. It should be kept in mind that if the axial surface of a fold is inclined, the hinge will migrate laterally with depth, and the hinge is generally the part of the fold having the maximum curvature. There are numerous folds in the Raton basin that could have excellent fracture systems. It is necessary to determine the areas of maximum curvature of the shale interval having brittle interbeds capable of fracturing.

Carbonate-rich beds of the Greenhorn Limestone and Niobrara Formation appear to be the most widespread and thickest intervals that might develop fracture reservoirs. Siltstone or orthoquartzitic interbeds in the Graneros, Carlile, and Pierre Shales may provide other zones with fracture systems. Hydrocarbon shows have been reported from the Graneros, Greenhorn, Niobrara, and Pierre Formations in the New Mexico parts of the Raton basin. Also, minor gas was produced from the Garcia field near Trinidad, Colorado. Fracturing appears to have enhanced the reservoir characteristics of the Wagon Mound Dakota gas field in the southern part of the basin.

Structure contour maps and lithofacies maps showing brittle interbeds in dominantly shaly sequences are the basic tools used in exploration for fracture reservoirs. These maps for the Raton basin indicate numerous exploration targets.

WORONICK, R. E. and L. S. LAND, Univ. Texas at Austin, Austin, TX

Burial Cements in Lower Cretaceous Pearsall Formation and Lower Glen Rose Formation, South Texas

Lower Cretaceous platform carbonates and shales were buried to depths in excess of 2,000 ft (610 m) by the end of Eocene time, and were locally affected by late-stage cementation. Burial diagenetic cements include ferroan baroque dolomite, ferroan and nonferroan calcite, anhydrite, kaolinite, barytocelestite, galena, and sphalerite. The lack of these minerals in outcrop and their occurrence in fractures are evidence for a subsurface origin.

Carbonate cements are chemically and isotopically zoned; the $FeCO_3$ content in baroque dolomite cement varies by as much as 10 wt. % across a single crystal. Stratigraphic and regional distribution of iron in baroque dolomite indicates that the iron is derived from local sources. Good negative correlation between $\delta^{13}C$ values and iron contents of baroque dolomite suggests the